THE JOURNAL OF BIOLOGICAL CHEMISTRY VOL. 286, NO. 46, pp. 39871–39881, November 18, 2011

Osteopontin Signals through Calcium and Nuclear Factor of Activated T Cells (NFAT) in Osteoclasts

A NOVEL RGD-DEPENDENT PATHWAY PROMOTING CELL SURVIVAL[*][S]

Received for publication, August 19, 2011 Published, JBC Papers in Press, September 22, 2011, DOI 10.1074/jbc.M111.295048

Natsuko Tanabe[‡§1], **Benjamin D. Wheal**[¶], **Jiyun Kwon**[‡], **Hong H. Chen**[‖], **Ryan P. P. Shugg**[‡2], **Stephen M. Sims**[‡], **Harvey A. Goldberg**[‖], **and S. Jeffrey Dixon**[‡3]

From the [‡]*Department of Physiology and Pharmacology and the* [‖]*Department of Dentistry, Schulich School of Medicine and Dentistry,* [¶]*Graduate Program in Neuroscience, The University of Western Ontario, London N6A5C1, Canada and the* [§]*Nihon University School of Dentistry, Tokyo 101-0062, Japan*

Background: The extracellular matrix protein osteopontin enhances bone resorption by osteoclasts.
Results: Osteopontin induces oscillations in the concentration of cytosolic calcium in osteoclasts, leading to nuclear translocation of transcription factor NFATc1 and increased survival.
Conclusion: Osteopontin enhances osteoclast survival through a calcium-NFAT-dependent pathway.
Significance: This novel mechanism explains in part the stimulatory effects of osteopontin on bone resorption.

Osteopontin (OPN), an integrin-binding extracellular matrix glycoprotein, enhances osteoclast activity; however, its mechanisms of action are elusive. The Ca^{2+}-dependent transcription factor NFATc1 is essential for osteoclast differentiation. We assessed the effects of OPN on NFATc1, which translocates to nuclei upon activation. Osteoclasts from neonatal rabbits and rats were plated on coverslips, uncoated or coated with OPN or bovine albumin. OPN enhanced the proportion of osteoclasts exhibiting nuclear NFATc1. An RGD-containing, integrin-blocking peptide prevented the translocation of NFATc1 induced by OPN. Moreover, mutant OPN lacking RGD failed to induce translocation of NFATc1. Thus, activation of NFATc1 is dependent on integrin binding through RGD. Using fluorescence imaging, OPN was found to increase the proportion of osteoclasts exhibiting transient elevations in cytosolic Ca^{2+} (oscillations). OPN also enhanced osteoclast survival. The intracellular Ca^{2+} chelator 1,2-bis(*O*-aminophenoxy)ethane-*N*,*N*,*N*′,*N*′-tetraacetic acid (BAPTA) suppressed Ca^{2+} oscillations and inhibited increases in NFATc1 translocation and survival induced by OPN. Furthermore, a specific, cell-permeable peptide inhibitor of NFAT activation blocked the effects of OPN on NFATc1 translocation and osteoclast survival. This is the first demonstration that OPN activates NFATc1 and enhances osteoclast survival through a Ca^{2+}-NFAT-dependent pathway. Increased NFATc1 activity and enhanced osteoclast survival may account for the stimulatory effects of OPN on osteoclast function *in vivo*.

Osteopontin (OPN)[4] is a major noncollagenous protein of bone that is also found in the extracellular matrix of other mineralized tissues and in body fluids. OPN is rich in aspartic acid, glutamic acid, and serine, and can be post-translationally modified by phosphorylation, glycosylation, sulfation, proteolysis, and cross-linking (1). In bone, OPN is produced by osteoblasts, osteocytes, macrophages, and osteoclasts (2). By binding to mineral, OPN can regulate biomineralization, directly inhibiting the *de novo* formation of hydroxyapatite (3) and the growth of calcium oxalate crystals (4). OPN binds to cells through integrin and nonintegrin receptors. An RGD sequence in OPN is responsible for binding to several integrins including $\alpha v\beta 3$. Other integrins such as $\alpha 9\beta 1$ can bind in an RGD-independent manner to the SVVYGLR motif in human OPN (or to SLAYGLR in rat and mouse OPN), which is located in the thrombin-cleaved N-terminal fragment of OPN (5). OPN also binds to the adhesion receptor CD44 in an RGD-independent manner (6). By acting through integrins and CD44, OPN induces a number of functional effects including chemotaxis of macrophages and other cell types, cytoprotection, and regulation of T helper type 1 cells (1). As well, OPN is expressed in many cancers, where it is thought to promote invasion and metastasis, and elevated levels of OPN have been associated with poor prognosis (7).

There are some reports describing signaling pathways activated by OPN. In Bcr-Abl-expressing leukemia cells, OPN induces degradation of IκB, the inhibitor of NF-κB (8). Moreover, OPN activates phosphatidylinositol 3-kinase/Akt signaling in pro-B-cell lines (9). Although many functions have been identified, relatively little is known about how OPN signals downstream of integrins and CD44 to exert its pleiotropic effects in multiple cell types.

* This work was supported by the Canadian Institutes of Health Research (CIHR).
[S] The on-line version of this article (available at http://www.jbc.org) contains supplemental Figs. S1–S3 and Videos S1–S3.
[1] Supported in part by the Sato Fund, Nihon University School of Dentistry, Tokyo, Japan.
[2] Recipient of a Frederick Banting and Charles Best Canada Graduate Scholarship from the CIHR.
[3] To whom correspondence should be addressed. E-mail: jeff.dixon@schulich.uwo.ca.

[4] The abbreviations used are: OPN, osteopontin; BAPTA-AM, 1,2-bis(*O*-aminophenoxy)ethane-*N*,*N*,*N*′,*N*′-tetraacetic acid-acetoxymethyl ester; BzATP, 2′,3′-*O*-(4-benzoylbenzoyl)-ATP; M199, medium 199; NFATc1, nuclear factor of activated T-cells cytoplasmic 1; nOPN, native osteopontin; OPN-KAE, OPN in which Arg-Gly-Asp was mutated to Lys-Ala-Glu; RANKL, receptor activator of nuclear factor κB ligand; TRP, transient receptor potential.

Osteoclasts are large multinucleated cells with the unique capability for extracellular resorption of the mineralized matrices of bone, teeth, and mineralized cartilage (10). The resorbing osteoclast seals to the bone surface in a region of the cell known as the clear zone, characterized by the presence of an annular actin ring that encompasses a specialized membrane known as the ruffled border. Protons, transported across the ruffled border, dissolve bone mineral, whereas secreted enzymes such as cathepsin K degrade organic components of the matrix. OPN has been shown to colocalize with the $\alpha v\beta 3$ integrin in the clear zone of actively resorbing osteoclasts (11), leading to the suggestion that OPN functions as an "anchor" by attaching the osteoclast to the bone mineral. Moreover, both osteoclast attachment to bone and subsequent resorption can be blocked by antibodies directed against $\alpha v\beta 3$ or OPN, or by soluble RGD-containing peptides or RGD mimetics (12, 13). In general, OPN-deficient ($OPN^{-/-}$) mice display normal skeletal development and bone structure (14); however, in contrast to control mice, $OPN^{-/-}$ mice are resistant to bone resorption induced by ovariectomy (15). In addition, OPN is required for the efficient resorption of ectopically implanted bone (16) and for enhanced resorption induced by reduced mechanical strain *in vivo* (17).

In osteoclasts, signaling by OPN through the $\alpha v\beta 3$ integrin is thought to involve activation of the tyrosine kinase Pyk2, c-Src, phosphatidylinositol 3-kinase, and phospholipase Cγ (18, 19). Either activation of phospholipase Cγ (causing release of Ca^{2+} from intracellular stores) or Ca^{2+} influx through channels would lead to elevation in the concentration of cytosolic free calcium ($[Ca^{2+}]_i$). In this regard, Pyk2 is activated by rise of $[Ca^{2+}]_i$, suggesting that OPN induces elevation of $[Ca^{2+}]_i$. However, it was previously reported that soluble OPN actually induces a decrease of $[Ca^{2+}]_i$ in osteoclasts (20). To resolve this paradox, one of the goals of the present study was to examine the effect of immobilized OPN on $[Ca^{2+}]_i$ in osteoclasts.

Members of the nuclear factor of activated T cells (NFAT) family of transcription factors control diverse cellular processes. Inactive NFATc proteins are maintained in the cytoplasm in a hyperphosphorylated state. Activation of NFATc proteins involves several steps (21). Ca^{2+} signaling activates the phosphatase calcineurin, which dephosphorylates multiple serine residues on NFATc proteins. Dephosphorylation induces a conformational change that exposes a nuclear localization signal, leading to the translocation of NFATc to nuclei and regulation of transcription (22). NFATc1 is strongly induced during the stimulation of osteoclast differentiation by RANKL (receptor activator of nuclear factor κB ligand). Moreover, NFATc1 has been shown to be essential for osteoclastogenesis (23). In cooperation with other factors such as AP-1, NFAT targets a number of genes involved in osteoclast activation and function, including those encoding osteoclast-associated receptor (OSCAR), $\beta 3$ integrin, cathepsin K, tartrate-resistant acid phosphatase, and the dendritic cell-specific transmembrane protein DC-STAMP (22). In the present study, we investigated the possible involvement of calcium-NFAT signaling in mediating the actions of OPN on osteoclasts.

We discovered that immobilized OPN acts through an RGD-dependent receptor to increase the number of osteoclasts exhibiting oscillations in $[Ca^{2+}]_i$, which in turn induces nuclear translocation of NFATc1. Moreover, we show for the first time that OPN enhances osteoclast survival and that this effect is mediated by a calcium-NFAT-dependent pathway. This novel mechanism explains in part the stimulatory effects of OPN on resorptive function *in vivo*.

EXPERIMENTAL PROCEDURES

Materials—Medium 199 (M199) buffered with 25 mM HEPES and 26 mM HCO_3^- (catalog number 12340), M199 buffered with 25 mM HEPES and 4 mM HCO_3^- (catalog number 12350), heat-inactivated fetal bovine serum (FBS), antibiotic solution (penicillin, 10,000 units/ml; streptomycin, 10,000 μg/ml; and amphotericin B, 25 μg/ml), Alexa Fluor 488 phalloidin, fura-2 acetoxymethyl ester (AM), Hoechst 33342, and BAPTA-AM were purchased from Invitrogen. Bovine albumin (BSA) (crystallized) was from ICN Biomedicals Inc. (Irvine, CA). Mounting medium (VectaShield) was from Vector Laboratories (Burlingame, CA). GRGDTP and GRADTP peptides were from Sigma and Calbiochem (La Jolla, CA), respectively. UTP and 2′,3′-*O*-(4-benzoylbenzoyl)-ATP (BzATP) were from Sigma. U73122 was from Enzo Life Sciences (Plymouth Meeting, PA). The cell-permeable peptide inhibitor of NFAT activation, 11R-VIVIT (RRRRRRRRRRR-GGG-MAGPHPVIVITG-PHEE), and the inactive control peptide 11R-VEET (RRRRRRRRRRR-GGG-MAGPPHIVEETGPHVI) (24) were custom synthesized and purified by Invitrogen.

Preparation of Recombinant, Mutant, and Native Forms of Osteopontin—Rat recombinant OPN (OPN, prokaryotically expressed without post-translational modifications) was obtained as described previously (25). Briefly, N-terminal His-tagged full-length OPN was prepared by cloning rat OPN cDNA (residues 17–301 lacking the signal sequence) into a pET-28a(+) expression vector (Novagen, EMD Biosciences, Darmstadt, Germany), which was used to transform *Escherichia coli* BL21 cells. The recombinant protein was purified by nickel affinity chromatography and fast protein liquid chromatography. The purified protein was subjected to amino acid analysis and selected samples were analyzed by matrix-assisted laser desorption ionization time-of-flight mass spectrometry, giving a relative molecular mass of 36,100 (26). OPN in which Arg-Gly-Asp (RGD) was mutated to Lys-Ala-Glu (KAE) (OPN-KAE) was prepared using the QuikChange™ Site-directed Mutagenesis System (Stratagene).

Native OPN (nOPN, post-translationally modified) was isolated from adult rat long bones and purified as described previously (27). Briefly, bones were washed with phosphate-buffered saline (PBS) containing proteinase inhibitors, then ground with a mortar and pestle under liquid nitrogen. The resulting powder was treated with 4 M guanidine-HCl to remove nonmineral-associated proteins and then treated with 0.5 M EDTA. The EDTA extract was concentrated by ultrafiltration, subjected to buffer exchange, and fractionated by fast protein liquid chromatography. Purified nOPN was analyzed by matrix-assisted laser desorption ionization time-of-flight mass spectrometry and an average relative molecular mass of 37,600 was determined.

Substrate Preparation and Osteoclast Isolation—Glass coverslips (12-mm diameter) or glass-bottomed culture dishes (35-mm diameter, MatTek, Ashland MA) were uncoated or precoated with OPN, nOPN, or BSA as follows. Each coverslip or dish was coated with 150 or 250 μl, respectively, of protein solution (20 μg/ml in PBS, unless otherwise indicated) and left for 2 h at room temperature. The remaining solution was removed prior to plating of osteoclast suspensions.

Osteoclasts were isolated from the long bones of neonatal Wistar rats or New Zealand White rabbits as described previously (28). All procedures were approved by the Council on Animal Care of The University of Western Ontario and were in accordance with the guidelines of the Canadian Council on Animal Care. Briefly, long bones were dissected free of soft tissue and minced with a scalpel in M199 buffered with HEPES (25 mM) and HCO_3^- (26 mM) supplemented with 15% FBS and 1% antibiotic solution. The resulting cells were suspended by repeated passage through a glass pipette. Where indicated, test substances were added to the cell suspension, which was then plated on coverslips or glass-bottomed dishes. Following plating, osteoclasts were incubated at 37 °C in 5% CO_2 for 1 h, and then cultures were gently washed with PBS to remove nonadherent cells and incubated in fresh medium for 0.5–2 h before use.

Assessment of Osteoclast Morphology—Samples were fixed with paraformaldehyde (4%) in sucrose solution (2%) for 10 min at room temperature, washed 2 times with PBS, and then permeabilized with 0.1% Triton X-100 in PBS for 10 min at room temperature. Following two 5-min washes with PBS, cells were incubated in 1% BSA for 30 min at room temperature, stained for filamentous actin using 66 nM Alexa Fluor 488-phalloidin for 20 min at room temperature, and washed two times with PBS. Cells were visualized using an Axioplan 2 fluorescence microscope with a Plan Neofluar ×20/0.5 NA objective (Zeiss, Jena, Germany). Spreading was quantified by tracing the perimeter of each osteoclast to obtain mean planar cell area under each condition using ImageMaster software (Photon Technology International, Birmingham, NJ).

Immunofluorescence Localization of NFATc1—Rabbit osteoclasts were plated on coated or uncoated glass coverslips for the indicated time. Cells were fixed with paraformaldehyde (4%) in sucrose solution (2%), permeabilized with Triton X-100, and blocked with normal goat serum. We used a mouse monoclonal antibody (7A6, catalog number sc-7294, Santa Cruz Biotechnology) established to be specific for NFATc1 (29). Staining was completed with a biotinylated anti-mouse IgG and fluorescein-conjugated streptavidin (Vector Laboratories). We assessed localization of fluorescent label in all osteoclasts on each coverslip (usually 140–200 cells per coverslip) using an LSM 510 confocal microscope (Zeiss). In some experiments, nuclei were stained with 4′,6-diamidino-2-phenylindole (DAPI, Vector Laboratories); in others, selected samples were processed without primary antibody. Osteoclasts were rated positive for nuclear localization if the fluorescence intensity of the nuclei exceeded that of the cytoplasm. The proportion of osteoclasts exhibiting nuclear localization was then calculated. To account for differences in control NFATc1 activity in separate osteoclast preparations, data were normalized as a fraction of the control value.

Monitoring of $[Ca^{2+}]_i$ by Digital Fluorescence Imaging—Isolated rat osteoclasts were plated on BSA- or OPN-coated glass-bottomed culture dishes. Following a 1-h incubation and washing, cells were loaded with fura-2 by incubation with 1.5 μM fura-2 AM for 45 min in supplemented M199 buffered with HEPES (25 mM) and HCO_3^- (26 mM) at 37 °C in 5% CO_2. Medium was then replaced with supplemented M199 buffered with HEPES (25 mM) and HCO_3^- (4 mM). Dishes were placed in a stage warmer (35 °C) mounted on a Nikon microscope (Nikon Eclipse TE2000-U, Tokyo, Japan). Osteoclasts were imaged using a Plan Fluor ×20/0.45 NA for phase-contrast or Plan Fluor ×40/1.3 oil/water immersion objective for fluorescence. Cells were excited with alternating wavelengths of 345/380 nm using a DeltaRam system (Photon Technology International) and the emission was acquired using a bandpass filter (510 ± 20 nm) (30). Ratio images were acquired every 6 s with a Cascade Photometrics 650 cooled charge-coupled device camera (653 × 492 pixels; Roper Scientific Inc., Tucson, AZ) and ImageMaster software. Where indicated, soluble test substances were applied locally to cells by pressure ejection from a micropipette. Measurements of $[Ca^{2+}]_i$ pose technical challenges due to the thin and variable profile of osteoclasts and their changing shape. The ratio of fluorescence intensity at 345/380 nm gives an index of $[Ca^{2+}]_i$ and reliably conveys the frequency and time course of Ca^{2+} transients. We did not attempt to calibrate the ratio, due to factors such as inhomogeneity of dye and Ca^{2+} within the cells.

Quantification of Osteoclast Survival and Apoptosis—Rat osteoclasts were isolated and plated on coated or uncoated coverslips and incubated at 37 °C in 5% CO_2 for 1 h in supplemented M199 buffered with HEPES (25 mM) and HCO_3^- (26 mM). Coverslips were then washed gently with PBS to remove nonadherent cells and incubated for an additional 0.5–1 h. Osteoclasts were then counted using phase-contrast microscopy as described previously (31). Cultures were incubated for an additional 18 h at 37 °C in 5% CO_2. The number of osteoclasts per coverslip was counted again, and survival was expressed as the proportion of the initial osteoclast number on the same coverslip. Data were then normalized as a fraction of control. In this series of experiments, the initial number of osteoclasts per coverslip was 64 ± 38 (mean ± S.D., n = 173 coverslips).

To examine apoptosis, rat osteoclasts were plated on coated or uncoated glass-bottomed dishes in supplemented M199 buffered with HEPES (25 mM) and HCO_3^- (26 mM) and incubated at 37 °C in 5% CO_2 for 1 h. Coverslips were then washed gently with PBS to remove nonadherent cells. Cultures were incubated for an additional 6 h at 37 °C in 5% CO_2 and then stained with the vital DNA dye Hoechst 33342 (5 μg/ml, for at least 10 min). Nuclear morphology was examined using an Axio Observer Z1 fluorescence microscope with a Plan Neofluar ×40/1.3 NA objective (Zeiss). Osteoclasts exhibiting condensed and/or fragmented nuclei were scored as apoptotic (32). Apoptosis was quantified as the number of apoptotic osteoclasts expressed as a proportion of the total number of oste-

oclasts in the same dish. Data were then normalized as a fraction of control.

Statistical Analyses—Unless otherwise indicated, each independent experiment was performed in triplicate; *n* indicates the number of independent experiments. Differences between two groups were evaluated by *t* tests. Differences among three or more groups were evaluated by one-way analysis of variance followed by Dunnett's multiple comparisons test. Differences in the proportion of osteoclasts exhibiting oscillations in $[Ca^{2+}]_i$ were evaluated by chi-square test. Differences were accepted as statistically significant at $p < 0.05$.

RESULTS

Osteopontin Promotes Osteoclast Spreading—In avian osteoclast-like cells, OPN has been found to stimulate spreading and motility (33). To confirm the activity of our rat recombinant OPN, we examined its effects on the morphology of isolated rat osteoclasts. Osteoclasts were plated on OPN-coated or uncoated glass coverslips for 2 h, fixed, and labeled with fluorescently tagged phalloidin to reveal filamentous actin. Osteoclasts plated on OPN displayed markedly enhanced spreading compared with cells on uncoated glass (supplemental Fig. S1, *A* and *B*). Moreover, osteoclasts on OPN exhibited larger lamellipodia and enhanced labeling of peripheral ruffles. Quantification revealed that the planar area of osteoclasts on OPN was significantly larger than the area of control osteoclasts on uncoated glass (supplemental Fig. S1*C*). Thus, interaction of osteoclasts with OPN enhances spreading, reflecting activation of underlying signaling pathways, which we went on to study.

OPN Enhances Nuclear Localization of NFATc1 in Osteoclasts—NFATc transcription factors are activated initially by the Ca^{2+}/calmodulin-dependent protein phosphatase, calcineurin. NFATc1 is strongly induced during RANKL-stimulated osteoclast differentiation (23) and we have shown that NFAT signaling mediates in part the stimulatory effects of RANKL on osteoclast survival (34). We used immunofluorescence to monitor the spatial distribution of NFATc1, which accumulates in the nuclei upon activation (supplemental Fig. S2). To investigate the effects of OPN, rabbit osteoclasts were plated on uncoated coverslips (Control) or coverslips coated with OPN and incubated for 1.5 to 24 h. OPN enhanced nuclear translocation of NFATc1, with the greatest effect evident at 3 h after plating (Fig. 1*A*).

We next compared NFATc1 translocation in osteoclasts plated for 3 h on a control substrate, on OPN (which lacks post-translational modifications), or on native rat OPN (nOPN, post-translationally modified). OPN and nOPN enhanced nuclear localization of NFATc1 to a similar extent (Fig. 1, *B* and *C*).[5] In contrast to the effects of OPN and nOPN, BSA did not significantly affect localization of NFATc1 (normalized values

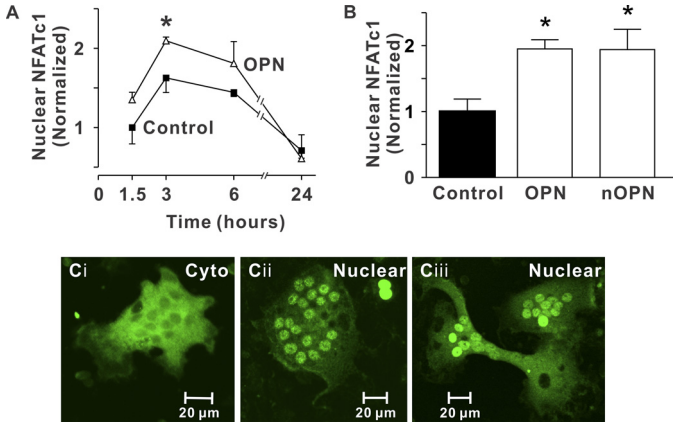

FIGURE 1. **Nuclear accumulation of NFATc1 induced by OPN.** Glass coverslips were uncoated (*Control*) or coated with recombinant OPN (*OPN*) or native OPN (*nOPN*) as indicated. *A,* rabbit osteoclasts were incubated for 1.5 to 24 h. Preparations were then fixed and NFATc1 localization was assessed by immunofluorescence. Data are the proportion of osteoclasts exhibiting nuclear localization of NFATc1, expressed as a fraction of the control value at 1.5 h (mean ± S.E., $n = 3$ independent experiments). *, $p < 0.05$ compared with the control value at the same time. *B,* rabbit osteoclasts were plated on the indicated substrates and fixed after 3 h. The histogram shows the proportion of osteoclasts exhibiting nuclear localization of NFATc1. Data are expressed as a fraction of control and are mean ± S.E., $n = 6$ independent experiments. *, $p < 0.05$ compared with control (in this series of experiments, 19 ± 3% of osteoclasts exhibited nuclear localization of NFATc1 on uncoated (*Control*) surfaces). *C, i,* image of a osteoclast plated on an uncoated coverslip showing predominantly cytoplasmic (Cyto) NFATc1 localization. *ii* and *iii*, images of osteoclasts plated on recombinant OPN (*ii*) and native OPN (*iii*) showing NFATc1 localized predominantly in the nuclei (*Nuclear*). At least 2,430 osteoclasts were examined in each group.

of nuclear NFATc1 on BSA-coated substrates were 0.72 ± 0.28 compared with 1.00 ± 0.14 for osteoclasts on uncoated surfaces, $n = 3$ independent experiments). Taken together, these data establish that OPN increases nuclear localization of NFATc1 in osteoclasts, and that post-translational modifications are not essential for causing translocation of NFATc1.

Role of Integrins in the Nuclear Translocation of NFATc1 Induced by OPN—Osteoclasts express high levels of $\alpha v\beta 3$ integrin, which is thought to be an important regulator of resorptive activity (13). OPN is known to bind to $\alpha v\beta 3$ integrin in an RGD-dependent manner (12). Therefore, we examined the role of integrins in mediating the effect of OPN on NFATc1 localization, first using the RGD-containing, integrin-blocking sextapeptide GRGDTP and the RAD-containing, inactive control peptide GRADTP. Rabbit osteoclasts were treated with vehicle, RAD, or RGD peptide prior to plating on uncoated glass (Control) or on OPN-coated glass. Three hours following plating, osteoclasts were fixed and NFATc1 localization was assessed. Whereas, OPN induced robust nuclear accumulation of NFATc1 in osteoclasts treated with vehicle (Fig. 2*A*), treatment with the integrin-blocking peptide abolished the effect of OPN on NFATc1 activation. In contrast, the RAD-containing, control peptide had no significant effect on the distribution of NFATc1.

Next, we compared the effects of OPN to mutated OPN lacking the integrin binding domain (OPN-KAE), prepared by replacing Arg-Gly-Asp (RGD) with Lys-Ala-Glu (KAE). Consistent with the effect of the integrin-blocking peptide, OPN-KAE failed to induce nuclear accumulation of NFATc1 in osteoclasts (Fig. 2*B*). Together, these findings show that OPN-

[5] To examine the possibility that differences between unmodified OPN and native OPN may be observed at a coating concentration lower than the 20 μg/ml used in this study, we repeated these experiments using a coating concentration of 5 μg/ml. At this concentration, there was no significant effect of either unmodified or native OPN (when normalized as a fraction of control, values of nuclear NFATc1 on unmodified OPN-coated substrates were 0.90 ± 0.29 compared with 1.08 ± 0.18 for osteoclasts on native OPN-coated substrates, $n = 3$ independent experiments).

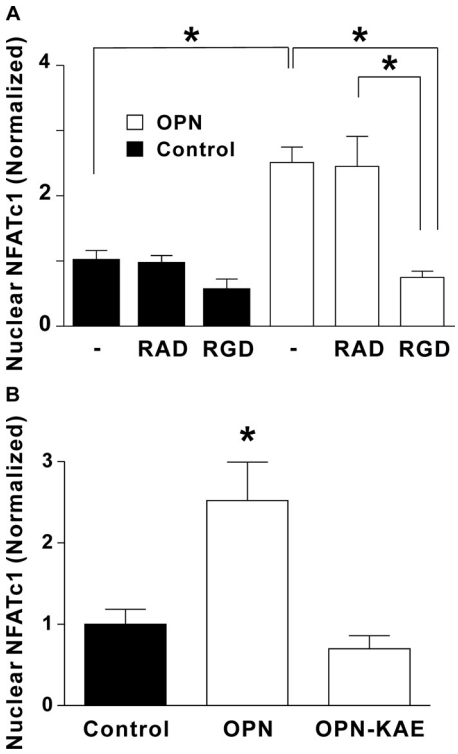

FIGURE 2. **Role of integrins in nuclear translocation of NFATc1 induced by OPN: effects of the RGD-containing peptide and the RGD-mutant form of OPN.** *A,* rabbit osteoclasts suspended in supplemented M199 buffered with HEPES (25 mM) and HCO_3^- (26 mM) were treated with the integrin-blocking sextapeptide GRGDTP (*RGD*, 50 μg/ml), the inactive control peptide GRADTP (*RAD*, 50 μg/ml), or vehicle (–). Cells were then plated on coverslips coated with OPN or on uncoated glass (*Control*). After a 3-h incubation at 37 °C in 5% CO_2, osteoclasts were fixed and NFATc1 localization was assessed using immunofluorescence. The histogram shows the proportion of osteoclasts exhibiting nuclear localization of NFATc1. Data are expressed as a fraction of vehicle-treated control and are mean ± S.E., $n = 4–7$ independent experiments, *, $p < 0.01$. *B,* rabbit osteoclasts were plated on uncoated glass (*Control*) or coverslips coated with OPN or OPN without the integrin binding domain (*OPN-KAE*). After a 3-h incubation, NFATc1 localization was assessed using immunofluorescence. The histogram shows the proportion of osteoclasts exhibiting nuclear localization of NFATc1. Data are expressed as a fraction of control and are mean ± S.E., $n = 3$ independent experiments, *, $p < 0.01$ compared with control.

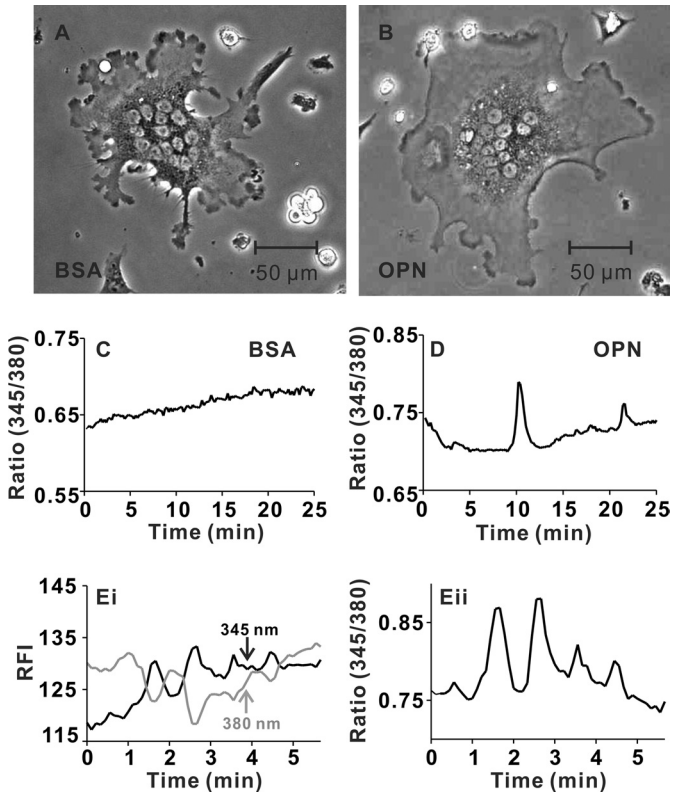

FIGURE 3. **OPN enhances calcium oscillations in osteoclasts.** Rat osteoclasts were plated on glass-bottomed culture dishes coated with BSA or OPN. Cells were loaded with fura-2 and bathed in supplemented M199 buffered with HEPES (25 mM) and HCO_3^- (4 mM). Dishes were placed in a stage warmer (35 °C) and osteoclasts were imaged using alternating excitation wavelengths of 345/380 nm. Fluorescence images were acquired every 6 s with a charge-coupled device camera. *A,* representative phase-contrast image of osteoclast plated on BSA. *B,* representative phase-contrast image of osteoclast plated on OPN. *C,* representative trace of the fluorescence ratio at 345/380 nm for a single osteoclast plated on BSA. In this case, oscillations in $[Ca^{2+}]_i$ were not observed. Ratio images are available as supplemental Video S1. *D,* representative trace from a region of a single osteoclast plated on OPN. In this case, 2 transient elevations in $[Ca^{2+}]_i$ were observed. Ratio images are available as supplemental Video S2. *E, i,* fluorescence intensities at 345 and 380 nm excitation are plotted as a function of time for another osteoclast plated on OPN. Increases in the signal at 345 nm coincided with decreases in intensity at 380 nm, consistent with authentic changes in $[Ca^{2+}]_i$. *E, ii,* fluorescence ratio for the cell illustrated in *i*. Data are based on responses from a total of 25–26 osteoclasts for each substrate, from 6 independent experiments.

induced activation of NFATc1 is dependent on integrin binding to the RGD motif.

Osteopontin Increases the Proportion of Osteoclasts Exhibiting Oscillations of $[Ca^{2+}]_i$—Because NFATc1 is activated by the Ca^{2+}-dependent protein phosphatase calcineurin, we investigated the effects of immobilized OPN on $[Ca^{2+}]_i$ in osteoclasts. Cells plated on BSA-coated or OPN-coated coverslips (Fig. 3, *A* and *B*) were monitored using digital fluorescence imaging. Diversity in patterns of cytosolic Ca^{2+} was apparent, with some osteoclasts having stable, unchanging $[Ca^{2+}]_i$ (Fig. 3*C*), and others exhibiting prominent Ca^{2+} transients (Fig. 3*D*) that were often spatially restricted to localized regions of the cell (supplemental Videos S1 and S2 illustrate the 345/380 nm ratios of osteoclasts on BSA and OPN). The frequency of multiple Ca^{2+} elevations (referred to as oscillations) was variable with a mean of ~0.2 transients per min. When the relative fluorescence intensities at 345 and 380 nm excitation were plotted for a series of typical oscillations, the signal at 345 nm increased concomitantly with a decrease in intensity at 380 nm (Fig. 3*E*). These data are consistent with authentic changes in $[Ca^{2+}]_i$ and rule out the possibility that oscillations in the ratio arose from nonspecific changes in fluorescence intensities.

We next quantified the number of osteoclasts exhibiting oscillations in $[Ca^{2+}]_i$. The criteria for Ca^{2+} oscillations were: 1) a series of at least 2 transient elevations in the 345/380 ratio over a period of 25 min, and 2) the amplitude of each transient must have been at least 2 times that of baseline fluctuations in the 345/380 ratio. A greater proportion of osteoclasts exhibited oscillations when plated on OPN compared with BSA (16 of 26 cells on OPN compared with 7 of 25 cells plated on BSA, significantly different based on χ^2 test, $p = 0.016$) (Table 1). Thus, OPN stimulates regional elevations of $[Ca^{2+}]_i$ in osteoclasts, a phenomenon that may underlie its ability to activate NFATc1 in these cells.

To examine the effects of soluble OPN on $[Ca^{2+}]_i$ in osteoclasts, cells were plated on BSA-coated coverslips and moni-

TABLE 1

Effect of OPN on the number of osteoclasts exhibiting oscillations in $[Ca^{2+}]_i$

Rat osteoclasts were plated on coverslips coated with BSA or OPN and loaded with fura-2 as described under "Experimental Procedures." Individual osteoclasts were monitored for periods of at least 25 min. Data show the number of osteoclasts exhibiting oscillations in $[Ca^{2+}]_i$, which were defined as a series of at least 2 transient elevations in the 345/380 ratio of amplitude at least 2 times that of the maximum level of baseline fluctuations. A greater proportion of osteoclasts exhibited oscillations when plated on OPN compared to BSA (significantly different based on chi-square test, $p < 0.05$). Data are based on responses from a total of 25–26 osteoclasts for each condition from 6 independent preparations of cells.

Substrate	Oscillations	No oscillations	Proportion of osteoclasts exhibiting oscillations
BSA	7	18	28%
OPN	16	10	62%

tored using digital fluorescence imaging. Soluble OPN (20 μg/ml) applied focally to osteoclasts using a micropipette had no effect on $[Ca^{2+}]_i$ (Fig. 4*A*). As a positive control, osteoclasts were stimulated with BzATP, an agonist at the P2X7 receptor found on osteoclasts (28). The P2X7 receptor is an ATP-gated cation channel that, upon activation, permits Ca^{2+} influx (35). BzATP (100 μM) applied focally to osteoclasts using a micropipette induced robust transient elevations of $[Ca^{2+}]_i$ (Fig. 4*B*). In contrast to the regional Ca^{2+} elevations induced by immobilized OPN (supplemental Video S2), BzATP induced global elevations of $[Ca^{2+}]_i$ (supplemental Video S3). Thus, even though we observed $[Ca^{2+}]_i$ elevations induced by soluble agonists such as BzATP, no detectable responses were induced by soluble OPN.

Effects of OPN on Osteoclast Survival and Apoptosis—Cell survival is a key factor that regulates the number of osteoclasts and hence bone resorption *in vivo* (36). Therefore, we examined the effect of OPN on osteoclast survival. Rat osteoclasts were plated on uncoated coverslips (Control) or on coverslips coated with BSA or OPN. Survival was quantified by counting the number of osteoclasts before and after an 18-h incubation period and calculating the proportion of surviving cells. Osteoclasts were identified by phase-contrast microscopy as multinucleated cells (≥3 nuclei). OPN markedly enhanced osteoclast survival (Fig. 5*A*). In contrast, BSA had no significant effect. These data establish that OPN regulates osteoclast survival.

To investigate the mechanism by which OPN enhances survival, we evaluated osteoclast apoptosis. Apoptosis in osteoclasts is characterized by nuclear condensation and fragmentation, usually occurring in all nuclei simultaneously (37). We visualized nuclear morphology using the membrane-permeant dye Hoechst 33342. Apoptotic osteoclasts exhibited condensed and fragmented nuclei, clearly distinguishable from the nuclear morphology in nonapoptotic cells (supplemental Fig. S3). In keeping with the survival data, osteoclasts plated on OPN, but not BSA, showed significantly reduced apoptosis (Fig. 5*B*). These data are consistent with OPN enhancing survival through the suppression of apoptosis.

Essential Role for Ca^{2+} Signaling in OPN-induced Activation of NFATc1 and Enhancement of Osteoclast Survival—We next investigated the role of Ca^{2+} oscillations in mediating the effects of OPN on NFATc1 localization and osteoclast survival. Cells were loaded with the cytosolic Ca^{2+} chelator BAPTA, using conditions that, we have shown previously, abolish transient elevations of $[Ca^{2+}]_i$ in osteoclasts induced by RANKL or ATP (38). We first confirmed the effectiveness of BAPTA in suppressing Ca^{2+} oscillations in rat osteoclasts plated on OPN. Osteoclasts exhibiting robust oscillations were treated with

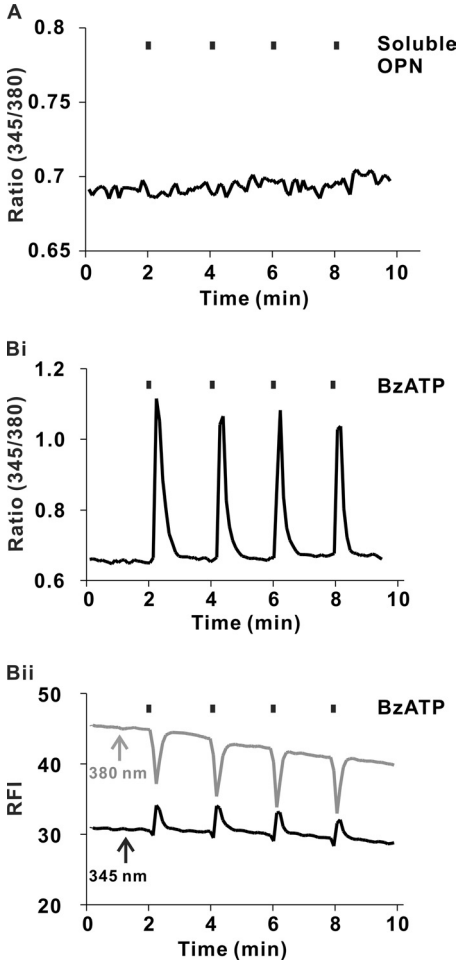

FIGURE 4. **Effects of soluble OPN and P2X7 agonist BzATP on $[Ca^{2+}]_i$ in osteoclasts.** Rat osteoclasts were plated on glass-bottomed culture dishes coated with bovine albumin. Cells were loaded with fura-2 and imaged using alternating excitation wavelengths of 345/380 nm. Test substances were applied by pressure ejection from a micropipette, at the times indicated by the *vertical bars above* the traces. *A,* trace of the fluorescence ratio at 345/380 nm for a single osteoclast stimulated repeatedly with soluble OPN (20 μg/ml in the micropipette). Changes in $[Ca^{2+}]_i$ were not observed. *Trace* is representative of 6 of 6 osteoclasts tested in 3 independent experiments. *B, i,* representative trace of the fluorescence ratio at 345/380 nm for a single osteoclast stimulated repeatedly with BzATP (100 μM in the micropipette). BzATP induced robust transient elevations in $[Ca^{2+}]_i$. Ratio images of these global $[Ca^{2+}]_i$ elevations are available as supplemental Video S3. *ii,* fluorescence intensities at 345 and 380 nm for the cell illustrated in *i* are plotted as a function of time. Increases in the signal at 345 nm coincided with decreases in intensity at 380 nm, consistent with authentic changes in $[Ca^{2+}]_i$. Data are representative of responses from 6 of 6 osteoclasts tested in 3 independent experiments.

BAPTA-AM (50 μM) or its vehicle. BAPTA abolished the oscillations in Ca^{2+} with little effect on resting levels of $[Ca^{2+}]_i$ (in 6 of 6 cells treated with BAPTA-AM, Fig. 6*A*). In contrast, oscillations were continued in rat osteoclasts plated on OPN and

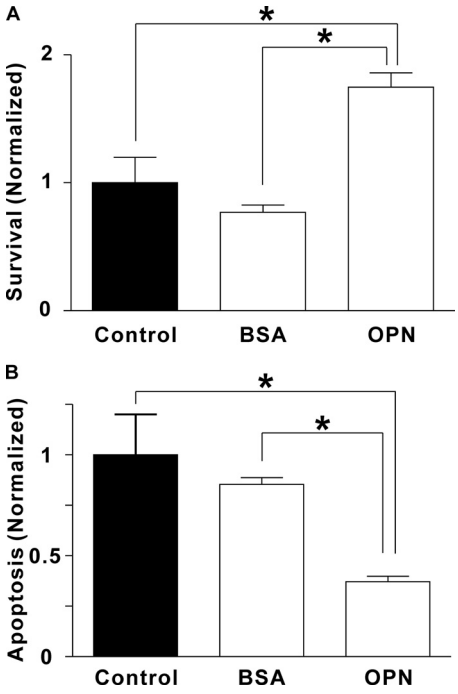

FIGURE 5. **Effects of OPN on osteoclast survival and apoptosis.** Rat osteoclasts were plated on uncoated glass (*Control*) or substrate coated with BSA or OPN in supplemented M199 buffered with HEPES (25 mM) and HCO_3^- (26 mM). After a 1-h incubation at 37 °C in 5% CO_2, preparations were washed to remove nonadherent cells. *A,* to quantify survival, we first incubated cultures for an additional 30 min to allow osteoclasts to spread. Osteoclasts were then counted, incubated 18 h at 37 °C in 5% CO_2, and then counted again. The number of surviving osteoclasts on each coverslip at 18 h was expressed as a percentage of the initial number of osteoclasts on the same coverslip. Data were then normalized as a fraction of the control value. Data are mean ± S.E., $n = 3$ independent experiments, *, $p < 0.05$. On uncoated (*Control*) surfaces, survival was 22 ± 4%. *B,* to assess apoptosis, osteoclasts were incubated for 6 h at 37 °C in 5% CO_2 and then stained with the DNA dye Hoechst 33342 (5 μg/ml, for at least 10 min). Osteoclasts exhibiting condensed and/or fragmented nuclei were scored as apoptotic (supplemental Fig. S3). The number of apoptotic osteoclasts was expressed as a percentage of the total number of osteoclasts in the same dish. Data were then normalized as a fraction of the control value. Data are mean ± S.E., $n = 3$ independent experiments, *, $p < 0.05$. On uncoated (*Control*) surfaces, apoptosis was 39 ± 8%.

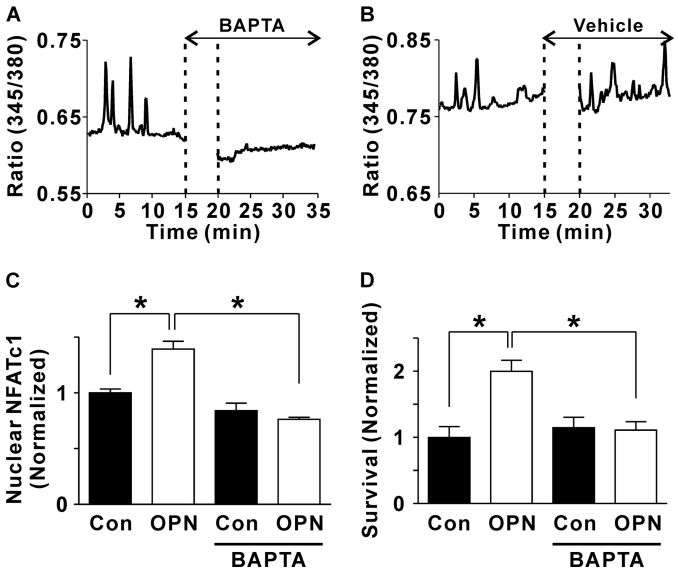

FIGURE 6. **Role of Ca^{2+} in mediating the effects of OPN on NFATc1 translocation and osteoclast survival: actions of the Ca^{2+} chelator BAPTA.** *A* and *B,* rat osteoclasts were plated on glass-bottomed culture dishes coated with OPN. Cells were loaded with fura-2 and imaged using alternating excitation wavelengths of 345/380 nm. Osteoclasts exhibiting robust oscillations were selected for further study. Illustrated are representative traces of the fluorescence ratio at 345/380 nm for single osteoclasts on OPN that were treated, where indicated, with BAPTA-AM (50 μM, *A*) or vehicle (*B*). BAPTA abolished the oscillations in $[Ca^{2+}]_i$ (in 6 of 6 osteoclasts studied from three independent experiments). In contrast, oscillations were continued in vehicle-treated osteoclasts (in 5 of 5 cells studied from three independent experiments). *C,* coverslips were uncoated (*Con*, control) or coated with OPN. Rabbit osteoclasts were plated on these substrates in the presence or absence of BAPTA-AM (50 μM). After a 1-h incubation at 37 °C in 5% CO_2, preparations were washed to remove nonadherent cells and BAPTA-AM. Cultures were incubated for an additional 2 h, fixed, and NFATc1 localization was assessed by immunofluorescence. The histogram shows the proportion of osteoclasts exhibiting nuclear localization of NFATc1. Data are expressed as a fraction of untreated control and are mean ± S.E., $n = 3$ independent experiments, *, $p < 0.01$. *D,* coverslips were uncoated (*Con*, control) or coated with OPN. Rat osteoclasts were plated on these substrates in the presence or absence of BAPTA-AM (50 μM). After a 1-h incubation at 37 °C in 5% CO_2, preparations were washed to remove nonadherent cells and BAPTA-AM. Survival was assessed by counting the number of osteoclasts before and after an additional 18 h of culture. The number of surviving osteoclasts on each coverslip at 18 h was expressed as a percentage of the initial number of osteoclasts on the same coverslip. Data were normalized as a fraction of the control value in cells not treated with BAPTA-AM. Data are mean ± S.E., $n = 3$ independent experiments each performed in triplicate, *, $p < 0.05$.

treated with vehicle (in 5 of 5 cells examined, Fig. 6*B*). Thus, BAPTA was effective in blocking OPN-induced Ca^{2+} oscillations.

To investigate the effects of BAPTA on NFATc1 localization, rabbit osteoclasts were plated on uncoated or OPN-coated substrates. Cells were then loaded with BAPTA by incubation with BAPTA-AM (50 μM) for 1 h. After a 3-h incubation, preparations were fixed and NFATc1 localization was assessed by immunofluorescence. BAPTA abolished the effect of OPN on NFATc1 translocation (Fig. 6*C*). In contrast, BAPTA had little effect on NFATc1 activation in osteoclasts on uncoated substrates. These data support the involvement of Ca^{2+} signaling in OPN-induced activation of NFATc1.

We further investigated the role of Ca^{2+} elevations in mediating the effects of OPN on cell survival. Rat osteoclasts were plated on uncoated or OPN-coated substrates and loaded with BAPTA by incubation with BAPTA-AM (50 μM) for 1 h. Survival was quantified by counting the number of osteoclasts before and after an 18-h incubation period. Like its effects on NFATc1 localization, BAPTA abolished the increase in osteoclast survival induced by OPN without affecting survival on the uncoated substrate (Fig. 6*D*). Thus, we established that both OPN-induced activation of NFATc1 and enhancement of survival are dependent on cytosolic Ca^{2+} signaling.

Role of NFAT in Mediating the Effects of OPN on Osteoclast Survival—We considered whether NFAT activation is required for the effects of OPN on osteoclast survival. To suppress NFAT signaling, we used a cell-permeable peptide (11R-VIVIT) that specifically inhibits NFAT activation by blocking its interaction with calcineurin (24). We first confirmed the inhibitory effect of 11R-VIVIT on OPN-induced NFATc1 activation as follows. Rabbit osteoclasts were preincubated for 15 min with vehicle or 11R-VIVIT, and then plated on uncoated or OPN-coated substrates in the continued presence of vehicle or 11R-VIVIT. After a 3-h incubation, preparations were fixed and NFATc1 localization was assessed by immunofluorescence. 11R-VIVIT abolished the effect of OPN on NFATc1 translocation (Fig. 7*A*); in contrast, it had only a small effect on NFATc1

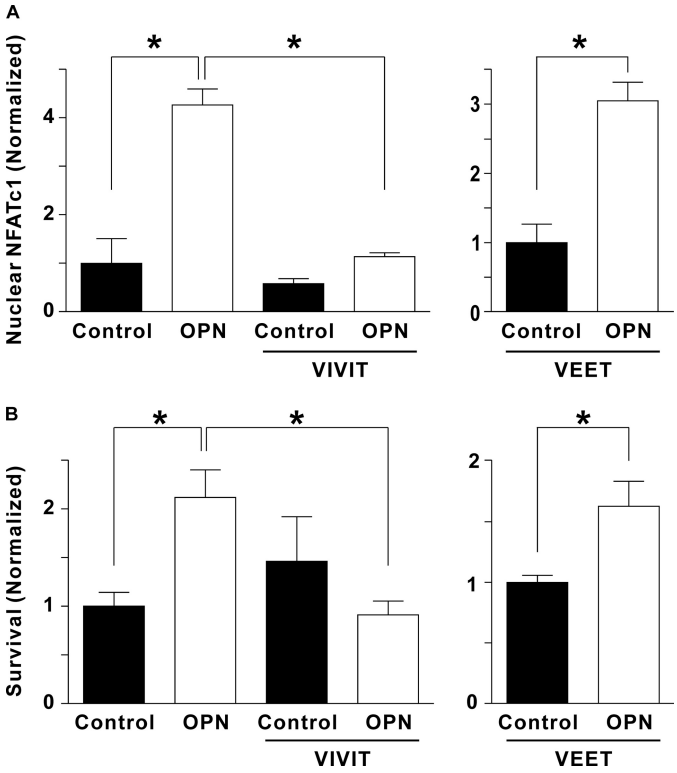

FIGURE 7. **The effects of 11R-VIVIT, a specific inhibitor of NFAT activation, on OPN-induced nuclear translocation of NFATc1 and osteoclast survival.** *A,* rabbit osteoclasts, suspended in supplemented M199 buffered with HEPES (25 mM) and HCO_3^- (26 mM) were treated with vehicle or 11R-VIVIT (*VIVIT*, 3 μM) for 15 min. In a separate series of experiments, cells were treated with the inactive control peptide 11R-VEET (*VEET*, 3 μM) for 15 min. Cells were then plated on uncoated glass (*Control*) or coverslips coated with OPN. After a 1-h incubation at 37 °C in 5% CO_2, preparations were washed and cultures were incubated for an additional 2 h in the continued presence of vehicle, 11R-VIVIT (VIVIT, 1 μM) or 11R-VEET (VEET, 1 μM). Preparations were then fixed and NFATc1 localization was assessed by immunofluorescence. Histograms show the proportion of osteoclasts exhibiting nuclear localization of NFATc1. Data are mean ± S.E., $n = 3$ independent experiments, *, $p < 0.01$. In the *left panel*, data are normalized as a fraction of vehicle-treated control; in the *right panel*, data are normalized as a fraction of control. *B,* rat osteoclasts, suspended in supplemented M199 buffered with HEPES (25 mM) and HCO_3^- (26 mM), were treated with vehicle or 11R-VIVIT (VIVIT, 3 μM) for 15 min. In a separate series of experiments, cells were treated with 11R-VEET (VEET, 3 μM) for 15 min. Cells were then plated on uncoated glass (*control*) or coverslips coated with OPN. After a 1-h incubation at 37 °C in 5% CO_2, preparations were washed. Survival was assessed by counting the number of osteoclasts before and after an additional 18 h of culture in the continued presence of vehicle, 11R-VIVIT (1 μM) or 11R-VEET (VEET, 1 μM). The number of surviving osteoclasts on each coverslip at 18 h was expressed as a percentage of the initial number of osteoclasts on the same coverslip. Data are mean ± S.E., $n = 3$ independent experiments, *, $p < 0.05$. In the *left panel*, data are normalized as a fraction of vehicle-treated control; in the *right panel*, data are normalized as a fraction of control.

localization in osteoclasts on uncoated substrates. These data establish that 11R-VIVIT effectively blocks OPN-induced activation of NFATc1 in osteoclasts.

To assess the role of NFAT activation in mediating the effects of OPN on osteoclast survival, rat osteoclasts were preincubated for 15 min with vehicle or 11R-VIVIT, and then plated on uncoated or OPN-coated substrates in the continued presence of vehicle or 11R-VIVIT. 11R-VIVIT suppressed the increase in osteoclast survival induced by OPN (Fig. 7*B*), establishing a role for NFAT in mediating the effects of OPN on survival.

To investigate possible nonspecific actions of 11R-VIVIT, we used the cell-permeable inactive control peptide 11R-VEET (24). OPN still induced significant increases in NFATc1 translocation and osteoclast survival in the presence of 11R-VEET (Fig. 7). These data are consistent with a specific inhibitory effect of 11R-VIVIT, thus supporting our conclusion that NFAT is activated by calcineurin and is necessary for the effects of OPN on osteoclast survival.

DISCUSSION

OPN is an important regulator of bone resorption (15–17); however, the mechanisms by which it promotes osteoclast activity have remained poorly understood. In this study, we report for the first time that OPN induces nuclear translocation of NFATc1 through an RGD-dependent mechanism. Moreover, OPN enhanced the proportion of osteoclasts exhibiting oscillations in $[Ca^{2+}]_i$ and blockade of these oscillations prevented OPN-induced translocation of NFATc1. Last, we report that OPN enhances osteoclast survival and that this pathway is dependent on both elevation of $[Ca^{2+}]_i$ and activation of NFAT. Signaling through this novel pathway may account for some of the effects of OPN on osteoclasts, as well as inflammatory and tumor cells.

Effects of OPN on Osteoclast Morphology and Spreading—We observed that, when plated on OPN, osteoclasts exhibited enhanced spreading and increased filamentous actin in the peripheral ruffles. These observations are in accord with those of Chellaiah and Hruska (33), who observed that soluble OPN stimulated the formation of actin filaments at the leading edge of migrating avian osteoclast-like cells. Interestingly, these effects were mimicked by RGD-containing peptides and blocked by an antibody directed against the $\alpha v\beta 3$ integrin. Similarly, it was reported recently that osteoclast-like cells differentiated from murine RAW 264.7 cells on OPN were more spread than cells formed on vitronectin or fibronectin (39). On the other hand, Teti and co-workers (40) reported that authentic rabbit osteoclasts plated on an OPN-coated substratum exhibited less spreading than cells plated on a control surface. Although the reason for this difference is not clear, we found in the present study that authentic osteoclasts plated on OPN displayed dramatically enhanced spreading, presumably arising from activation of intracellular signaling pathways.

OPN Activates NFATc1 in Osteoclasts—To the best of our knowledge, the present study is the first to demonstrate that OPN, in any cell type, stimulates intracellular signaling pathways leading to the nuclear translocation of NFAT. In osteoclast precursors, RANKL has been shown to induce activation of NFATc1, promoting osteoclast differentiation (23). As well, RANKL acts on mature osteoclasts to enhance their survival (41), an effect dependent in part on activation of NFAT (34). Moreover, NFAT stimulates the resorptive activity of mature osteoclasts (42, 43). High levels of cytosolic Ca^{2+} activate calmodulin, which in turn stimulates the phosphatase calcineurin leading to activation of the NFATc family of transcription factors. In the present study, we used 11R-VIVIT a peptide that binds to calcineurin, blocking its interaction with NFAT without affecting its ability to dephosphorylate other substrates (24). We found that 11R-VIVIT blocked the ability of OPN to activate NFATc1, implicating calcineurin in the pathway. Similarly, the intracellular Ca^{2+} chelator BAPTA blocked OPN-

induced activation of NFATc1. Although direct effects of OPN-induced NFAT activation on transcriptional regulation in osteoclasts have not yet been demonstrated, our observations establish that OPN activates the initial stages of Ca^{2+}-NFAT signaling.

Little is known about whether OPN stimulates NFAT signaling in other cell types. In this regard, the development and function of invariant natural killer T cells was found to be defective in $OPN^{-/-}$ mice (44). These defects were linked to impaired activation of NFATc1, leading to reduced production of IL-4. It is possible that, as in osteoclasts, OPN functions in an autocrine or paracrine manner in invariant natural killer T cells to activate NFATc1, an important signaling molecule downstream of antigen receptor activation in these cells.

OPN Structure-Activity Relationship—In the present study, we found that the ability of OPN to activate NFATc1 was absolutely dependent on the presence of the RGD domain. This observation was supported by the action of an RGD-containing peptide, which blocked OPN-induced NFATc1 translocation. These findings are in keeping with the ability of $\alpha v\beta 3$ integrins, which are highly expressed in osteoclasts, to bind to OPN in an RGD-dependent manner (12). Many of the effects of OPN on cellular function in other systems have been shown to be RGD dependent, although some OPN actions are mediated by CD44 (45) or CD11c/CD18 integrin (46), both of which are RGD independent. Interestingly, the effects of OPN on gastric tumor cells are mediated by binding to CD44, leading to inside-out signaling via Src and robust integrin activation (47). Thus, although we have shown that integrin signaling is essential for the actions of OPN on osteoclasts, the possibility exists that OPN activates both $\alpha v\beta 3$ integrins and CD44 and that cross-talk is required for downstream effects such as activation of NFATc1.

OPN is subject to multiple post-translational modifications, including phosphorylation, glycosylation, and sulfation and, in some cases, these modulate OPN-induced signaling (1, 45). Reported effects of post-translational modifications on the interaction of OPN with osteoclasts are varied, with some studies showing that post-translational modifications enhance osteoclast adhesion (48, 49) and others showing no effect on osteoclast attachment or actin ring formation (50). An explanation for these conflicting observations has been proposed based on differences in the concentration of OPN used to coat the substrate. Ek-Rylander and Andersson (49) found differences in osteoclast attachment to modified and unmodified OPN at coating concentrations ≤ 10 μg/ml; whereas, no effect was seen at the higher concentration of OPN (20 μg/ml) used by Razzouk and co-workers (50). We found no difference in the effects of recombinant OPN (lacking post-translational modifications) and native rat bone OPN (post-translationally modified) at either 5 or 20 μg/ml. Thus, post-translational modifications of OPN are not essential for inducing activation of NFATc1 in osteoclasts.

Immobilized OPN Regulates the Temporal Pattern of $[Ca^{2+}]_i$ in Osteoclasts—Previous studies of the effects of OPN and OPN-derived peptides on $[Ca^{2+}]_i$ in osteoclasts have yielded contradictory findings. Soluble OPN or RGD peptides were found to induce a prompt decrease in $[Ca^{2+}]_i$ in avian osteoclasts, responses that were blocked by an antibody directed against the $\alpha v\beta 3$ integrin (20). In contrast, application of soluble OPN or RGD peptides induced transient elevation of $[Ca^{2+}]_i$ in human osteoclast-like cells isolated from the giant cell tumor of bone (51). Consistent with these results, RGD-containing peptides were reported to induce transient elevation of $[Ca^{2+}]_i$ in isolated rat osteoclasts (52). These latter responses were most evident in osteoclast nuclei and were inhibited by an antibody directed against the integrin $\beta 3$ chain; however, a subsequent paper by the same group concluded that these responses were actually integrin independent (53). Thus, there is little consensus regarding the effects of OPN on Ca^{2+} signaling in osteoclasts or other cell types.

We did not observe any acute effect of soluble OPN on $[Ca^{2+}]_i$ in osteoclasts. However, we did find that a greater proportion of osteoclasts plated on OPN exhibited spontaneous oscillations in $[Ca^{2+}]_i$ than did cells plated on control substrates (glass or bovine albumin). In other cell types, oscillations in $[Ca^{2+}]_i$ regulate numerous functions, including secretion and gene transcription. In osteoclast precursors, it has been suggested that Ca^{2+} oscillations are required for activation of NFATc1, which is in turn necessary for osteoclast differentiation (23).

How might OPN stimulate Ca^{2+} oscillations in osteoclasts? Ligation of $\alpha v\beta 3$ integrins in osteoclasts leads to the phosphorylation and activation of phospholipase Cγ (18), which could lead to Ca^{2+} release from intracellular stores. This would explain stimulation of the Ca^{2+}-activated tyrosine kinase Pyk2 upon binding of $\alpha v\beta 3$. Alternatively, it was recently shown in bovine capillary endothelial cells that forces applied to integrins ($\beta 1$ in this case) rapidly activate Ca^{2+} influx through TRPV4 channels (54). Thus, it is conceivable that $\alpha v\beta 3$ integrins in osteoclasts also couple to activation of Ca^{2+}-permeable transient receptor potential (TRP) channels. In this regard, mice deficient in *Trpv4* exhibit impaired bone resorption; however, TRPV4-mediated Ca^{2+} influx is not thought to give rise to Ca^{2+} oscillations in osteoclasts (55). In initial studies, we have found that the phospholipase C inhibitor U73122 does not abolish Ca^{2+} oscillations in osteoclasts plated on OPN, although it does block P2Y-mediated elevation of $[Ca^{2+}]_i$ induced by UTP.[6] These findings support the possibility of Ca^{2+} influx through channels. The precise mechanism underlying OPN-regulated Ca^{2+} oscillations in osteoclasts is currently under investigation in our laboratory.

Enhancement of Osteoclast Survival through the Ca^{2+}-NFAT Pathway in Osteoclasts—Bone turnover *in vivo* is regulated by the differentiation of osteoclast precursors, the activation of mature osteoclasts, as well as the lifespan of osteoclasts (36). To the best of our knowledge, the present study is the first to demonstrate that OPN enhances osteoclast survival.

The predominant form of cell death for osteoclasts *in vitro* and *in vivo* is apoptosis (37). Several pathways may contribute to the effects of OPN on osteoclast apoptosis and survival. Ligation of $\alpha v\beta 3$ leads to "outside-in" signals that activate the phosphatidylinositol 3-kinase/Akt and Ras/ERK pathways (13, 56), both of which are linked to enhancement of survival. In addi-

[6] B. D. Wheal, S. J. Dixon, and S. M. Sims, unpublished observations.

tion, the present study shows that OPN enhances Ca^{2+} oscillations, leading to activation of NFATc1 that in turn is critical for survival signaling. In this regard, we have shown previously that suppression of $[Ca^{2+}]_i$ elevation using the intracellular Ca^{2+} chelator BAPTA abolished the ability of RANKL to enhance osteoclast survival (38). Although inhibition of NFAT signaling does not appear to affect osteoclast survival under basal conditions (43), studies using 11R-VIVIT showed that the stimulatory effects of RANKL on osteoclast survival were dependent in part on NFAT activation (34). More recently, we have shown that the ability of the potent lipid mediator, lysophosphatidic acid, to enhance osteoclast survival is also dependent on activation of NFAT (32). Thus, evidence is emerging for an important role of Ca^{2+}-NFAT signaling in the control of osteoclast survival by multiple factors.

Possible Role of the OPN-Ca^{2+}-NFAT Pathway in Vivo—In the present study, we have demonstrated that OPN signals through Ca^{2+}-NFAT to enhance osteoclast survival. Changes in osteoclast survival are thought to be an important mechanism regulating bone resorption *in vivo* (36). Therefore, OPN may act *in vivo* through the Ca^{2+}-NFAT pathway to promote osteoclast survival and thus increase bone resorption. As well, activation of NFAT has been shown to enhance the resorptive activity of mature osteoclasts (42, 43), a phenomenon that further explains the stimulatory effects of OPN on bone resorption *in vivo*. It is also possible that activation of Ca^{2+}-NFAT signaling contributes to the effects of OPN on tumor cells *in vivo*, as previous studies have implicated NFAT signaling in integrin-mediated carcinoma invasion (57) and in the invasive behavior of murine osteosarcoma (58).

Acknowledgments—We thank Dr. Graeme Hunter (The University of Western Ontario) for assistance with preparation of osteopontin. We also acknowledge the helpful advice and assistance of Matt Grol, Dr. Alexey Pereverzev, Elizabeth Pruski, and Tom Chrones (The University of Western Ontario), as well as the kind support of Dr. Masao Maeno (Nihon University School of Dentistry).

REFERENCES

1. Wang, K. X., and Denhardt, D. T. (2008) *Cytokine Growth Factor Rev.* **19,** 333–345
2. Heinegård, D., Andersson, G., and Reinholt, F. P. (1995) *Ann. N.Y. Acad. Sci.* **760,** 213–222
3. Boskey, A. L., Maresca, M., Ullrich, W., Doty, S. B., Butler, W. T., and Prince, C. W. (1993) *Bone Miner.* **22,** 147–159
4. Shiraga, H., Min, W., VanDusen, W. J., Clayman, M. D., Miner, D., Terrell, C. H., Sherbotie, J. R., Foreman, J. W., Przysiecki, C., Neilson, E. G., *et al.* (1992) *Proc. Natl. Acad. Sci. U.S.A.* **89,** 426–430
5. Yokosaki, Y., Matsuura, N., Sasaki, T., Murakami, I., Schneider, H., Higashiyama, S., Saitoh, Y., Yamakido, M., Taooka, Y., and Sheppard, D. (1999) *J. Biol. Chem.* **274,** 36328–36334
6. Weber, G. F., Ashkar, S., Glimcher, M. J., and Cantor, H. (1996) *Science* **271,** 509–512
7. Anborgh, P. H., Mutrie, J. C., Tuck, A. B., and Chambers, A. F. (2010) *J. Cell Mol. Med.* **14,** 2037–2044
8. Vejda, S., Piwocka, K., McKenna, S. L., and Cotter, T. G. (2005) *Br. J. Haematol.* **128,** 711–721
9. Lin, Y. H., and Yang-Yen, H. F. (2001) *J. Biol. Chem.* **276,** 46024–46030
10. Novack, D. V., and Teitelbaum, S. L. (2008) *Annu. Rev. Pathol.* **3,** 457–484
11. Reinholt, F. P., Hultenby, K., Oldberg, A., and Heinegård, D. (1990) *Proc. Natl. Acad. Sci. U.S.A.* **87,** 4473–4475
12. Ross, F. P., Chappel, J., Alvarez, J. I., Sander, D., Butler, W. T., Farach-Carson, M. C., Mintz, K. A., Robey, P. G., Teitelbaum, S. L., and Cheresh, D. A. (1993) *J. Biol. Chem.* **268,** 9901–9907
13. Nakamura, I., Duong, L. T., Rodan, S. B., and Rodan, G. A. (2007) *J. Bone Miner. Metab.* **25,** 337–344
14. Rittling, S. R., Matsumoto, H. N., McKee, M. D., Nanci, A., An, X. R., Novick, K. E., Kowalski, A. J., Noda, M., and Denhardt, D. T. (1998) *J. Bone Miner. Res.* **13,** 1101–1111
15. Yoshitake, H., Rittling, S. R., Denhardt, D. T., and Noda, M. (1999) *Proc. Natl. Acad. Sci. U.S.A.* **96,** 8156–8160
16. Asou, Y., Rittling, S. R., Yoshitake, H., Tsuji, K., Shinomiya, K., Nifuji, A., Denhardt, D. T., and Noda, M. (2001) *Endocrinology* **142,** 1325–1332
17. Ishijima, M., Rittling, S. R., Yamashita, T., Tsuji, K., Kurosawa, H., Nifuji, A., Denhardt, D. T., and Noda, M. (2001) *J. Exp. Med.* **193,** 399–404
18. Nakamura, I., Lipfert, L., Rodan, G. A., and Le, T. Duong (2001) *J. Cell Biol.* **152,** 361–373
19. Horne, W. C., Sanjay, A., Bruzzaniti, A., and Baron, R. (2005) *Immunol. Rev.* **208,** 106–125
20. Miyauchi, A., Alvarez, J., Greenfield, E. M., Teti, A., Grano, M., Colucci, S., Zambonin-Zallone, A., Ross, F. P., Teitelbaum, S. L., Cheresh, D., *et al.* (1991) *J. Biol. Chem.* **266,** 20369–20374
21. Rao, A., Luo, C., and Hogan, P. G. (1997) *Annu. Rev. Immunol.* **15,** 707–747
22. Sitara, D., and Aliprantis, A. O. (2010) *Immunol. Rev.* **233,** 286–300
23. Negishi-Koga, T., and Takayanagi, H. (2009) *Immunol. Rev.* **231,** 241–256
24. Noguchi, H., Matsushita, M., Okitsu, T., Moriwaki, A., Tomizawa, K., Kang, S., Li, S. T., Kobayashi, N., Matsumoto, S., Tanaka, K., Tanaka, N., and Matsui, H. (2004) *Nat. Med.* **10,** 305–309
25. da Silva, A. P., Ellen, R. P., Sørensen, E. S., Goldberg, H. A., Zohar, R., and Sodek, J. (2009) *Lab. Invest.* **89,** 1169–1181
26. Grohe, B., Taller, A., Vincent, P. L., Tieu, L. D., Rogers, K. A., Heiss, A., Sørensen, E. S., Mittler, S., Goldberg, H. A., and Hunter, G. K. (2009) *Langmuir* **25,** 11635–11646
27. Keykhosravani, M., Doherty-Kirby, A., Zhang, C., Brewer, D., Goldberg, H. A., Hunter, G. K., and Lajoie, G. (2005) *Biochemistry* **44,** 6990–7003
28. Naemsch, L. N., Dixon, S. J., and Sims, S. M. (2001) *J. Biol. Chem.* **276,** 39107–39114
29. Boss, V., Abbott, K. L., Wang, X. F., Pavlath, G. K., and Murphy, T. J. (1998) *J. Biol. Chem.* **273,** 19664–19671
30. Kovac, J. R., Chrones, T., and Sims, S. M. (2008) *Am. J. Physiol. Gastrointest Liver Physiol.* **294,** G88–98
31. Korcok, J., Raimundo, L. N., Du, X., Sims, S. M., and Dixon, S. J. (2005) *J. Biol. Chem.* **280,** 16909–16915
32. Lapierre, D. M., Tanabe, N., Pereverzev, A., Spencer, M., Shugg, R. P., Dixon, S. J., and Sims, S. M. (2010) *J. Biol. Chem.* **285,** 25792–25801
33. Chellaiah, M. A., and Hruska, K. A. (2003) *Calcif. Tissue Int.* **72,** 197–205
34. Pereverzev, A., Komarova, S. V., Korcok, J., Armstrong, S., Tremblay, G. B., Dixon, S. J., and Sims, S. M. (2008) *Bone* **42,** 150–161
35. Grol, M. W., Panupinthu, N., Korcok, J., Sims, S. M., and Dixon, S. J. (2009) *Purinergic Signal.* **5,** 205–221
36. Tanaka, S., Miyazaki, T., Fukuda, A., Akiyama, T., Kadono, Y., Wakeyama, H., Kono, S., Hoshikawa, S., Nakamura, M., Ohshima, Y., Hikita, A., Nakamura, I., and Nakamura, K. (2006) *Ann. N.Y. Acad. Sci.* **1068,** 180–186
37. Xing, L., and Boyce, B. F. (2005) *Biochem. Biophys. Res. Commun.* **328,** 709–720
38. Komarova, S. V., Pilkington, M. F., Weidema, A. F., Dixon, S. J., and Sims, S. M. (2003) *J. Biol. Chem.* **278,** 8286–8293
39. Gramoun, A., Goto, T., Nordström, T., Rotstein, O. D., Grinstein, S., Heersche, J. N., and Manolson, M. F. (2010) *J. Cell. Biochem.* **111,** 350–361
40. Teti, A., Taranta, A., Migliaccio, S., Degiorgi, A., Santandrea, E., Villanova, I., Faraggiana, T., Chellaiah, M., and Hruska, K. A. (1998) *J. Bone Miner. Res.* **13,** 50–58
41. Lacey, D. L., Tan, H. L., Lu, J., Kaufman, S., Van, G., Qiu, W., Rattan, A., Scully, S., Fletcher, F., Juan, T., Kelley, M., Burgess, T. L., Boyle, W. J., and Polverino, A. J. (2000) *Am. J. Pathol.* **157,** 435–448
42. Komarova, S. V., Pereverzev, A., Shum, J. W., Sims, S. M., and Dixon, S. J. (2005) *Proc. Natl. Acad. Sci. U.S.A.* **102,** 2643–2648

43. Ikeda, F., Nishimura, R., Matsubara, T., Hata, K., Reddy, S. V., and Yoneda, T. (2006) *J. Immunol.* **177,** 2384–2390
44. Diao, H., Iwabuchi, K., Li, L., Onoe, K., Van Kaer, L., Kon, S., Saito, Y., Morimoto, J., Denhardt, D. T., Rittling, S., and Uede, T. (2008) *Proc. Natl. Acad. Sci. U.S.A.* **105,** 15884–15889
45. Kazanecki, C. C., Uzwiak, D. J., and Denhardt, D. T. (2007) *J. Cell. Biochem.* **102,** 912–924
46. Schack, L., Stapulionis, R., Christensen, B., Kofod-Olsen, E., Skov Sørensen, U. B., Vorup-Jensen, T., Sørensen, E. S., and Höllsberg, P. (2009) *J. Immunol.* **182,** 6943–6950
47. Lee, J. L., Wang, M. J., Sudhir, P. R., Chen, G. D., Chi, C. W., and Chen, J. Y. (2007) *Cancer Res.* **67,** 2089–2097
48. Katayama, Y., House, C. M., Udagawa, N., Kazama, J. J., McFarland, R. J., Martin, T. J., and Findlay, D. M. (1998) *J. Cell. Physiol.* **176,** 179–187
49. Ek-Rylander, B., and Andersson, G. (2010) *Exp. Cell Res.* **316,** 443–451
50. Razzouk, S., Brunn, J. C., Qin, C., Tye, C. E., Goldberg, H. A., and Butler, W. T. (2002) *Bone* **30,** 40–47
51. Paniccia, R., Colucci, S., Grano, M., Serra, M., Zallone, A. Z., and Teti, A. (1993) *Am. J. Physiol. Cell Physiol.* **265,** C1289–C1297
52. Shankar, G., Davison, I., Helfrich, M. H., Mason, W. T., and Horton, M. A. (1993) *J. Cell Sci.* **105,** 61–68
53. Shankar, G., Gadek, T. R., Burdick, D. J., Davison, I., Mason, W. T., and Horton, M. A. (1995) *Exp. Cell Res.* **219,** 364–371
54. Matthews, B. D., Thodeti, C. K., Tytell, J. D., Mammoto, A., Overby, D. R., and Ingber, D. E. (2010) *Integr. Biol.* **2,** 435–442
55. Masuyama, R., Vriens, J., Voets, T., Karashima, Y., Owsianik, G., Vennekens, R., Lieben, L., Torrekens, S., Moermans, K., Vanden Bosch, A., Bouillon, R., Nilius, B., and Carmeliet, G. (2008) *Cell Metab.* **8,** 257–265
56. Del Fattore, A., Teti, A., and Rucci, N. (2008) *Arch. Biochem. Biophys.* **473,** 147–160
57. Jauliac, S., López-Rodriguez, C., Shaw, L. M., Brown, L. F., Rao, A., and Toker, A. (2002) *Nat. Cell Biol.* **4,** 540–544
58. Velupillai, P., Sung, C. K., Tian, Y., Dahl, J., Carroll, J., Bronson, R., and Benjamin, T. (2010) *PLoS Pathog.* **6,** e1000733